TITLE: Robust association between vascular habitats and patient prognosis in Glioblastoma: an international multicenter study

ABSTRACT:

Background: Glioblastoma is the most aggressive primary brain tumor characterized by a heterogeneous and abnormal vascularity. Vascular habitats within the enhanced tumor and the tumoral edema can be distinguished: High Angiogenic Tumor (HAT), Low Angiogenic Tumor (LAT), Infiltrated Peripheral Edema (IPE), and Vasogenic Peripheral Edema (VPE).

Purpose: To validate the association between hemodynamic markers from vascular habitats and overall survival (OS) in glioblastoma patients and the inter-center variability of MRI acquisition protocols.

Study type: multicenter retrospective study.

Population: 184 glioblastoma patients from seven European centers participating in the NCT03439332 clinical study.

Field Strength/Sequence: 1.5 (for 54 patients) or 3.0T (for 130 patients); Pre-gadolinium and post-gadolinium-based contrast agent-enhanced T1-weighted MRI, T2- and FLAIR T2-weighted and DSC T2* perfusion.

Assessment: Preoperative MRIs were analyzed to establish the association between the maximum relative Cerebral Blood Volume ($rCBV_{max}$) at the HAT, LAT, IPE and VPE habitats with OS. Moreover, the stratification capabilities of the hemodynamic markers to divide patients into long and short survivors were tested. The independence of the markers from the center acquisition was also assessed.

Statistical Tests: Uniparametric Cox regression. Kaplan-Meier test. Mann-Whitney test

Results: The $rCBV_{max}$ derived from the HAT, LAT and IPE habitats were significantly associated with patient OS ($p<0.05$; HR:1.05, 1.11, 1.28 respectively). Moreover, these markers can stratify patients into short and long survivors ($p<0.05$). The Mann-Whitney test found no significant differences among most of the centers, and no significant differences were observed in the Cox regression and Kaplan-Meier analyses among each of the participating centers.

Data Conclusion: The $rCBV_{max}$ calculated in HAT, LAT and IPE habitats is a clinically relevant prognostic biomarker for glioblastoma patients in the pre-treatment stage. This study demonstrates the relevance of the HTS habitats to assess the GBM vascular heterogeneity and their association with patient prognosis independently of the inter-center variability.

KEYWORDS: Glioblastoma; vascularity; perfusion DSC; overall survival; multicenter study

LIST OF ABBREVIATIONS:

- DSC: Dynamic Susceptibility Contrast
- GBM: Glioblastoma
- HAT: High Angiogenic Tumor
- IPE: Infiltrated Peripheral Edema
- LAT: Low Angiogenic Tumor
- MR: Magnetic Resonance
- MRI: Magnetic Resonance Imaging
- OS: Overall Survival
- $rCBV_{max}$: maximum relative Cerebral Blood Volume

- TE: Echo Time
- TR: Repetition Time
- ROI: Region of Interest
- VPE: Vasogenic Peripheral Edema

INTRODUCTION

Glioblastoma (GBM) is the most aggressive malignant primary brain tumor in adults and results in a median survival rate of 12-15 months (1, 2). It still carries a poor prognosis despite aggressive treatment, which includes tumor resection followed by chemo-radiotherapy (2-4).

One of the main factors thought to be responsible for GBM's aggressiveness is its vascular heterogeneity (4, 5), mainly defined by strong angiogenesis, which supplies the GBM's metabolic needs and accounts for its rapid progress (6, 7). The vascular profile of the tumor is strongly associated with the molecular characteristics of the lesion (7), which means that the vascular conditions of the early tumor stages and its environment are both associated with GBM progress (6).

The negative association between patient survival rates and vascular features extracted from perfusion MRI has been widely analyzed in the literature (4, 8, 9). In these studies, perfusion indices such as relative Cerebral Blood Volume (rCBV) or capillary heterogeneity were found to have prognostic capabilities. The methodologies employed to assess these perfusion indices range from manually defined ROIs, which introduce high uncertainty and lack repeatability, to more up-to-date techniques based on artificial intelligence methods able to analyze tumoral heterogeneity (10-15).

In 2018, Juan-Albarracín *et al*. (16) proposed the HTS methodology (freely accessible at ONCOhabitats site: https://www.oncohabitats.upv.es) to characterize GBM's vascular heterogeneity by means of delineating the vascular habitats. This technique, known as the Hemodynamic Tissue Signature (HTS), defines four habitats within the lesion with different hemodynamic behavior: The High Angiogenic Tumor (HAT) habitat, Low Angiogenic

Tumor (LAT) habitat, potentially Infiltrated Peripheral Edema (IPE) and the Vasogenic Peripheral Edema (VPE). This study found a significant correlation between overall survival (OS) and HTS markers in the high and low angiogenic habitats (16). In 2018, Fuster *et al*. demonstrated the ability of these imaging markers to improve the prognosis of conventional models based on clinical, morphological and demographic features (17), although both studies were performed on a limited number of patients from a single hospital.

Although both researchers and clinicians are increasingly demanding imaging markers for decision making (18), to validate them in clinical practice, two *translational gaps* have to be overcome (O'Connor *et al* (19)): the first is related to using preclinical or clinical datasets from a single or only a few expert centers. The second requires that multiple centers be involved in the study, together with the biological validation of the biomarkers. Although previous studies (16, 17) overcame the first translational gap, to validate the vascular markers from the HTS habitats, an extended multicenter study is needed.

This paper presents the preliminary results of the international retrospective multicenter study NCT03439332, registered at ClinicalTrial.gov (https://clinicaltrials.gov/ct2/show/NCT03439332). The study focuses on the validation of the association between GBM vascular heterogeneity described by the HTS habitats and the patient OS in a large heterogeneous international cohort and includes imaging and clinical profiling of 196 patients collected from clinical routines at 7 centers in 4 different countries.

MATERIALS AND METHODS

Patient selection

The following seven European clinical centers participated in the study: the Hospital Universitario de La Ribera, Alzira, Spain; Hospital de Manises, Manises, Spain; Hospital Clinic, Barcelona, Spain; Hospital Universitario Vall d'Hebron, Barcelona, Spain; Azienda Ospedaliero-Universitaria di Parma, Parma, Italy; Centre Hospitalier Universitaire de Liège, Liège, Belgium and the Oslo University Hospital, Oslo, Norway. A Material Transfer Agreement (MTA) was approved by all the participating centers and an acceptance report was issued by the Ethical Committee of each center. The *managing institution* review board also approved this retrospective study and the requirement for patient-informed consent was waived.

The inclusion criteria for patients participating in the study were: *(a)* adult patients (age > 18 y.o.) with histopathological confirmation of GBM diagnosed between January 1, 2012 and January 1, 2018; *(b)* access to the preoperative MRI studies, including: pre- and post-gadolinium T1-weighted, T2-weighted, FLuid-Attenuated Inversion Recovery (FLAIR) and Dynamic Susceptibility Contrast (DSC) T2*-weighted perfusion sequences; and *(c)* patients who underwent standard Stupp treatment (20) with a minimum survival of 30 days.

Magnetic Resonance Imaging

Standard-of-care MR examinations were obtained at 1.5-T or 3-T scanners. Pre-gadolinium and post-gadolinium-based contrast agent-enhanced T1-weighted MRI, as well as T2-weighted, FLAIR T2-weighted and DSC T2* perfusion MRI sequences were collected from each center participating in the study. Supporting Information Table S1 summarizes the MRI

acquisition protocols grouped by center, including the Magnetic Field Strength, Repetition Time, Echo Time, matrix size, slice thickness, Field of View and the number of temporal acquisitions of the perfusion MR sequence.

GBM vascular heterogeneity assessment through HTS habitats

The HTS methodology from the ONCOhabitats platform was used to analyze the MRI studies. This methodology is composed of four stages: *(1) Preprocessing*, which includes correction of common MRI artifacts such as magnetic field in homogeneities and noise, multi-modal registration, brain extraction and motion correction; *(2) GBM tissue segmentation*, which implements a state-of-the-art deep learning 3D Convolutional Neural Network (CNN) that segments the enhancing tumor, edema and necrosis tissues; *(3) DSC Perfusion Quantification*, which calculates the hemodynamic maps derived from the DSC perfusion sequence (relative Cerebral Blood Volume (rCBV), relative Cerebral Blood Flow (rCBF), Mean Transit Time (MTT) and K2 permeability; and *(4) Hemodynamic Tissue Signature map*, in which an automated unsupervised segmentation algorithm is employed to detect four habitats with different hemodynamic behavior types: the High Angiogenic Tumor (HAT) habitat, Low Angiogenic Tumor (LAT) habitat, potentially Infiltrated Peripheral Edema (IPE) and the Vasogenic Peripheral Edema (VPE) (see Figure 1). Following (21), we define the *HTS marker* as the maximum rCBV ($rCBV_{max}$) computed as the 95th percentile of the rCBV distribution within a habitat. The GBM vascular heterogeneity of all the patients is thus described by four HTS markers, one for each habitat.

Association between patient OS and HTS markers (whole cohort)

Cox proportional hazard regression analysis was used to measure the associations between patient OS and HTS markers. The Proportional Hazard Ratios (HR) with a 95% confidence interval was reported, as well as the associated p-values corrected for multiple hypothesis testing by the False Discovery Rate (FDR) method (α-level: .05).

Kaplan-Meier analyses were performed to study the stratification abilities of the HTS markers to divide the population into short and long-term survivals. The optimum cut-off threshold for each perfusion index and habitat was determined by the C-index method. The C-Indexes for the final cut-off thresholds were also reported. The log-rank test was used to determine any statistical differences between the estimated survival functions of the groups divided by the HTS markers.

Association between patient OS and HTS markers per center

The similarities between the HTS marker distributions among the clinical centers with different MRI protocols were evaluated to determine the degree of agreement in describing tumor vascular heterogeneity. To do so we conducted a pair-wise Mann-Whitney U test to compare the distributions of the HTS markers of each center, considering that p-values higher than 0.05 implied no significant differences between the HTS markers calculated for these centers.

As in the analyses for the whole cohort, Cox regression analyses were conducted to assess whether the association between patient OS and HTS markers differed among the centers. Kaplan-Meier analyses were performed after dividing the population of each center using the cut-offs for each HTS marker previously calculated for the whole cohort.

All the statistical analyses were performed on Matlab R2017b (MathWorks, Natick, Mas)

RESULTS

From the initial cohort, consisting of 196 GBM patients, four cases were excluded due to HTS processing errors; five cases were excluded due to noise or MR artifacts that precluded DSC quantification (gamma variate R^2 goodness of fit < 0.95); one case was excluded due to inability to differentiate between tumor vascularity and reactive meningeal enhancement; and two cases were excluded due to defective perfusion images.

The study finally included 184 patients. Supporting Information Table S2 gives the patients from each center. Those who were still alive during the study were considered as censored observations, the date of censorship being the last date of contact with the patient or, if this information was not available, the date of the last MRI exam. Table 1 summarizes the most important demographic and clinical characteristics of the studied population.

Association between patient OS and HTS markers (whole cohort)

Table 2 shows the Cox proportional hazard analysis between HTS markers and patient OS. A significant correlation was found between CBV_{max} at HAT, LAT and IPE habitats ($p<0.05$, FDR<0.05) and patient OS. Negative associations were also found between patient OS and the $rCBV_{max}$ in these habitats.

The Kaplan-Meier results are summarized in Table 3, including estimated optimal cut-off thresholds, number of patients per group, estimated C-index, median OS calculated per group, and log-rank test results (p-values). Significant OS differences between low and high $rCBV_{max}$ were found in HAT, LAT and IPE. Those with low $rCBV_{max}$ in these habitats presented a higher median survival rate.

The Kaplan-Meier curves for the populations divided by high and low $rCBV_{max}$ in the vascular habitats are shown in Figure 2. The ability of the HTS markers to stratify patients into short and long-term survivors can be seen to coincide with the vascularity within the habitats.

Association between patient OS and vascular habitats per center

No significant differences were found between the $rCBV_{max}$ values of the habitats in most of the centers ($P>0.05$) (see Supporting Information Tables S3.1, S3.2 and S3.3). This can be seen in the box-whisker diagram in Figure 3, which shows how the $rCBV_{max}$ intervals for each hospital overlap.

Table S4 shows the results of the Cox regression analysis, broken down by hospital, of the HTS markers that yielded a significant association with OS (Table 2). Figure 4 contains a graph of the results, showing an unambiguous overlap between confidence intervals for most of the centers, suggesting no significant differences among them in calculating HTS markers. The results of the association of HTS markers and OS per hospital are consistent with those obtained for the whole cohort.

The Kaplan-Meier plot shows the stratification of the population per hospital in high and low vascular GBMs, using the optimal C-index thresholds shown in Figure 5. For the sake of clarity, this Figure only gives the results of the HAT marker (i.e. the HTS marker in the HAT habitat), as this showed the clearest differences between the populations. Supporting Information Figures S1 and S2 show the Kaplan-Meier plots for the LAT and IPE markers, respectively.

DISCUSSION

This paper gives the complete results of the multicenter validation focused on the first hypothesis defined in the NCT03439332 clinical study. Using data from seven European centers, significant negative associations were found between patient OS and the HTS markers in the HAT, LAT and IPE habitats. These results agree with a previous study (16) in which significantly longer survival rates were found for patients with lower $rCBV_{max}$.

Overcoming the variability in calculating imaging markers is not easy. Other authors have pointed out the uncertain or low reproducibility of some MRI markers, especially across centers (18, 19, 22, 23). A manual definition of ROIs and the interpretation of images by several experts may be other sources of variability, making it difficult to validate new imaging markers (22).

Although the current study involved a cohort with large variations in terms of patient demographics, as well as image acquisition protocols (see Tables 1 and Supporting Information Table S1), we did not find any relevant differences among the distributions of the HTS markers calculated from MRIs from different centers. Only one center, the *Clinic de Barcelona,* was found to have significant differences with the HAT markers from other centers. These results suggest that the proposed method is robust against inter-center variability in calculating vascular habitat HTS markers. Furthermore, the results of the Cox and Kaplan-Meier analysis per center show a robust association between patient OS and the HTS markers, regardless of the center of origin. The proposed thresholds were also effective in stratifying patients from different centers into long and short-term survivors according to their vascular profile.

Having demonstrated the influence of early-stage vascularity on the prognosis of GBM patients, this important factor may now be considered in any clinical study that includes population randomization. Until now, this variable has not been considered in clinical studies, mainly due to the lack of a robust and valid method of processing MRIs acquired under different conditions (i.e. different MRI protocols). The authors consider that the HTS method will help to overcome the current limitations and improve patient recruitment and randomization by initiating a route map to avoid the second translational gap cited above (18).

The proposed method segments the enhancing tumor into two habitats with different vascular profiles (i.e. HAT and LAT). Since HAT is the most vascular region in the tumor, the HAT $rCBV_{max}$ is quite similar to $rCBV_{max}$ in the whole enhancing tumor. In this regard, the correlation between high perfusion values in the HAT habitat and short-term OS is compatible with previous studies (8, 24, 25) that found a relationship between the perfusion parameters in the enhancing tumor region and the patient's survival rates.

We also found that the LAT habitat in the enhancing tumor has a strong association with OS and high stratification abilities. Sawlani RN *et al.* in (26) suggested the potential of the mean rCBV of the enhancing tumor as a predictive marker. The mean rCBV values obtained here for the whole tumor are comparable with the $rCBV_{max}$ in the LAT habitat. In 2005, Hambardzumyan & Bergers defined different GBM niches based on different cell constituents and the functional status of the vasculature (27). They distinguished between the perivascular niche, with vigorous and abnormal angiogenesis leading to a heterogeneous organization of blood vessels, and the hypoxic niche, with lower blood volume and flow values. Even though these regions could be consistent with the HAT and LAT habitats

proposed here, we have gone a step further and identified a new important region within the tumor which provides automatic reproducibility in calculating valuable prognostic imaging markers.

One of the most important of the present findings is the correlation found between long-term OS and low $rCBV_{max}$ in the IPE habitat. Edematous tissue has received much less attention than the active tumor in previous studies, although there is evidence that the vascularity in this area can influence tumor evolution and patient prognosis (28). In 2014, Jain R *et al*. (8) showed that the edema rCBV generally provided relevant prognostic information. Artzi*et al*. (28) described differences between the vasogenic and peripheral edema at the metabolic and vascular levels (28), while we found the HTS method can automatically delineate the infiltrated edema area, i.e. IPE. The clinical implications of this ability are given by the strong association between the IPE marker, patient prognosis, and the ability to stratify patients into long and short-term survivors, opening up new pre-surgical treatment options.

Since the influence of the molecular markers on patient prognosis has been demonstrated (1, 29), it may be of interest to add them as cofactors in survival models. The present multicenter study focused on the robustness of the HTS markers in dealing with images from multiple centers. In future studies we hope to analyze the possible association between molecular and imaging markers and their prognostic possibilities.

The HTS method is freely available at: https://www.oncohabitats.upv.es for use by research groups.

REFERENCES

1. Louis N, Perry A, Reifenberge RG, *et al*. The 2016 World Health Organization classification of tumors of the central nervous system: A summary. Acta Neuropathology. 2016; 131

2. Gately L, McLachlan SA, Dowling A, *et al*. Life beyond a diagnosis of glioblastoma: a systematic review of the literature. J Cancer Surviv. 2017; 11(4)

3. Bae S, Choi YS, Chang JH*et al*. Radiomic MRI Phenotyping of Glioblastoma: Improving Survival Prediction. Radiology. 2018; 289(3)

4. Akbari H, Macyszyn L, Da X*et al*. Pattern Analysis of Dynamic Susceptibility Contrast-enhanced MR Imaging Demonstrates Peritumoral Tissue Heterogeneity. Radiology. 2014; 273(2)

5. Soeda A, Hara A, Kunisada T, *et al*. The Evidence of Glioblastoma Heterogeneity. Scientific Reports. 2015; 5(7979)

6. Weis SM,& Cheresh DA. Tumor angiogenesis: molecular pathways and therapeutic targets. Nat Med. 2011; 17(11)

7. De Palma M, Biziato D, Petrova TV*et al.*Microenviromental regulation of tumour angiogenesis. Nature Reviews Cancer. 2017; 17(8)

8. Jain R, Poisson LM, Gutman D *et al*. Outcome Prediction in Patients with Glioblastoma by Using Imaging, Clinical, and Genomic Biomarkers: Focus on the Non-enhancing Component of the Tumor. Radiology.2014; 272(2); 484-93

9. Jensen RL, Mumert ML, Gillespie DL, Kinney AY, Schabel MC and Salzman KL. Preoperative dynamic contrast-enhanced MRI correlates with molecular markers of hypoxia and vascularity in specific areas of intratumoral microenvironment and is predictive of patient outcome. Neuro Oncol. 2014;16(2)

10. Fuster-Garcia E, García-Gómez JM *et al*. Imaging biomarkers. In: Martí-Bonmatí L, Alberich-Bayarri A, eds. Development and Clinical Integration. Switzerland: Springer International Publishing. 2017; 181-194

11. Demerath T, Simon-Gabriel CP, Kellner E, *et al*. Mesoscopic imaging of glioblastomas: Are diffusion, perfusion and spectroscopic measures influenced by the radiogenetic phenotype. Neuroradiology Journal. 2017; 30(1); 36-47

12. Jena A, Taneja S, Gambhir A, *et al*. Glioma recurrence versus radiation necrosis: Single-session multiparametric approach using simultaneous O-(2-18f-Fluoroethyl)-L-tyrosine PET/MRI. Clin Nucl Med. 2016; 41(5); 228-236

13. Price SJ, Young Adam MH, Scotton William J, *et al*. Multimodal MRI can identify perfusion and metabolic changes in the invasive margin of glioblastomas. J Magn Reson Imaging. 2016; 43(2); 487-494

14. Chang Y-CC, Ackerstaff E, Tschudi Y, et al. Delineation of tumor habitats based on dynamic contrast enhanced MRI. Sci Rep. 2017; 7(1); 9746

15. Cui Y, Tha KK, Terasaka S *et al*. Prognostic imaging biomarkers in glioblastoma: Development and independent validation on the basis of multi-region and quantitative analysis of MR images. Radiology. 2016; 278(2); 546-553

16. Juan-Albarracín J, Fuster-García E, Pérez-Girbés *et al*. Glioblastoma: Vascular Habitats Detected at Preoperative Dynamic Susceptibility-weighted Contrast-enhanced Perfusion MR Imaging Predict Survival. Radiology. 2018; 287(3)

17. Fuster-García E, Juan-Albarracín J, García-Ferrando GA*et al.*Improving the estimation of prognosis for glioblastoma patients by MR based hemodynamic tissue signatures. NMR in Biomedicine. 2018

18. Abramson RG, Burton KR, Yu JJ *et al*. Methods and Challenges in Quantitative Imaging Biomarker Development. Acad Radiol. 2015; 22(1)

19. O'Connor JPB, Aboagye EO, Adams JE *et al.* Imaging biomarker roadmap for cancer studies. Nature Reviews Clinical Oncology. 2016; 14

20. Stupp R, Mason WP, van den Bent MJ *et al.* Radiotherapy plus concomitant and adjuvant temozolomide for glioblastoma. N Engl J Med. 2005; 352(10)

21. Wetzel SG, Cha S, Johnson G *et al*. Relative cerebral blood volume measurements in intra cranial mass lesions: interobserver and intra observer reproducibility study. Radiology. 2002; 224(3)

22. Schnack HG, van Haren NEM, Hulshof Pol HE *et al*. Reliability of Brain Volumes from Multicenter MRI Acquisition: A Calibration Study. Human Brain Mapping. 2004; 22

23. De Guio F, Jouvent E, Biessels GJ *et al.* Reproducibility and variability of quantitative magnetic resonance imaging markers in cerebral small vessel disease. Journal of Cerebral Blood Flow & Metabolism. 2016; 36(8)

24. Liu TT, Achrol AS, Mitchell LA *et al.* Magnetic resonance perfusion image features uncover an angiogenic subgroup of glioblastoma patients with poor survival and better response to antiangiogenic treatment. Neuro-Oncology. 2017; 19(7)

25. Hirai T, Murakami R, Nakamura H *et al.* Prognostic value of perfusion MR imaging of high-grade astrocytomas: Long-term follow-up study. Am J Neuroradiol. 2008;2 9(8)

26. Sawlani RN, Raizer J, Horowitz SW *et al*. Glioblastoma: A Method for Predicting Response to Angiogenic Chemotherapy by Using MR Perfusion Imaging – Pilot Study. Radiology. 2010; 255(2)

27. Hambardzumyan D & Bergers G. Glioblastoma: Defining Tumor Niches. Trends Cancer. 2015; 1(4)

28. Artzi M, Bokstein F, Blumenthal DT *et al.* Differentiation between vasogenic-edema versus tumor-infiltrative area in patients with glioblastoma during bevacizumab therapy: a longitudinal MRI study. Eur J Radiol. 2014; 83(7)

29. Verhaak RG, Hoadley KA, Purdom E *et al*. Integrated genomic analysis identifies clinically relevant subtypes of glioblastoma characterized by abnormalities in PDGFRA, IDH1, EGFR, and NF1. Cancer Cell. 2010; 17(1)

Table 1: Demographic and clinical data of the 184 patients included in the study.

	H Ribera[a]	H Manises[b]	C Barcelona[c]	H Vall d'Hebron[d]	AO Parma[e]	CH Liège[f]	Oslo UH[g]	Total
GENDER (F/M)								
- # of patients	6/1	5/9	10/15	14/19	12/28	11/22	8/24	66/118
AGE AT DIAGNOSIS (years)								
- Mean	49	65	56	60	61	58	63	60
- Range	[24,67]	[39,79]	[35,74]	[30,81]	[35,76]	[32,77]	[40,81]	[24,81]
SURVIVAL (months)								
- Mean	14.6	14.4	10.3	15.2	11.7	15.3	15.4	13.7
- Median	9.1	12.8	9.6	13.0	12.9	14.5	12.6	12.6
- Range	[3.4,52.6]	[3.4,38.4]	[1.3,26.9]	[4.1,40.0]	[1.1,30.7]	[2.5,41.0]	[3.0,36.9]	[1.1,52.6]
RESECTION (# of patients)								
- Total	3	3	0	12	19	22	11	70
- Sub-total	1	4	10	10	15	6	21	67
- Biopsy	1	7	6	11	2	5	0	32
- Unknown	2	0	9	0	4	0	0	15
TUMOR LOCATION (# of patients)								
-Frontal	2	4	7	10	18	11	12	64
-Parietal	2	0	5	7	4	9	3	30
-Temporal	3	7	11	13	12	9	14	69
-Occipital	0	2	1	2	2	0	1	8
-Other /Unknown	0	1	1	1	4	4	2	13
IDH1								
-Mutated	2	0	4	0	0	0	1	6
-Wild type	2	0	4	32	30	34	31	99
-Unknown	3	14	17	1	10	0	1	79

Hospital de la Ribera[a]; Hospital de Manises[b]; Clinic de Barcelona[c]; Hospital Vall d'Hebron[d]; Azienda Ospedaliero-Universitaria di Parma[e]; Centre Hospitalier Universitaire de Liège[f]; Oslo University Hospital[g]

Table 2: Cox regression analysis for $rCBV_{max}$ of the vascular habitats to predict overall patient survival. * Indicates significant difference ($p<0.05$).

HTS MARKERS	HAZARD RATIO	95% CONFIDENCE INTERVAL	P-VALUE	P-VALUE (FDR ADJUSTED)
HAT	1.05	[1.01, 1.09]	**0.0115***	**0.0174***
LAT	1.11	[1.02, 1.20]	**0.0131***	**0.0174***
IPE	1.28	[1.05, 1.55]	**0.0122***	**0.0174***
VPE	1.19	[0.89, 1.60]	0.2502	0.2502

HTS: Hemodynamic Tissue Signature; HAT: High Angiogenic Tumor; LAT: Low Angiogenic Tumor; IPE: Infiltrated Peripheral Edema; VPE: Vasogenic Peripheral Edema

Table 3: Kaplan Meier and Log Rank test results for $rCBV_{max}$ in HAT, LAT, IPE and VPE to stratify patient in groups by low and high vascularity.

HTS MARKERS	CUT-OFF THRESHOLD	PATIENTS PER GROUP	AUC (C-INDEX)	MEDIAN OS PER GROUP	P-VALUE (LOG-RANK TEST)
$rCBV_{max}$		**Low High**		**Low High**	
HAT	11.06	[97, 87]	0.606	[14.3, 11.3]	**0.0014***
LAT	5.31	[91, 93]	0.605	[13.9, 11.3]	**0.0085***
IPE	1.92	[59 125]	0.634	[14.3, 11.4]	**0.0101***
VPE	1.67	[100, 84]	0.599	[13.8, 11.2]	0.1356

HTS: Hemodynamic Tissue Signature; $rCBV_{max}$: Maximum relative Cerebral Blood Volume; HAT: High Angiogenic Tumor; LAT: Low Angiogenic Tumor; IPE: Infiltrated Peripheral Edema; VPE: Vasogenic Peripheral Edema; AUC: Area under the curve

FIGURES

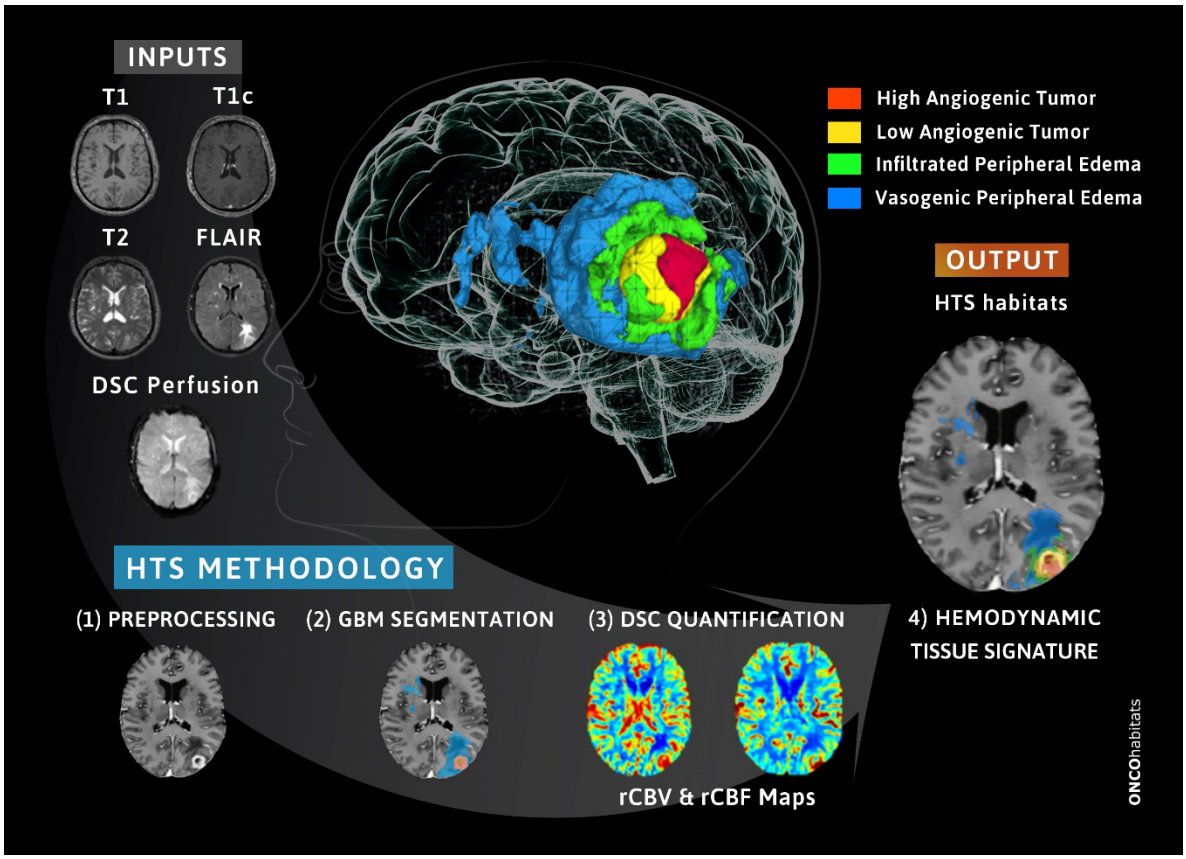

Figure 1: Hemodynamic Tissue Signature (HTS) methodology: (1): Preprocessing; (2): Segmentation; (3): DSC Perfusion Quantification; (4): Hemodynamic Tissue Signature. High Angiogenic Tumor (HAT), Low Angiogenic Tumor (LAT), Infiltrated Peripheral Edema (IPE), and Vasogenic Peripheral Edema (VPE).

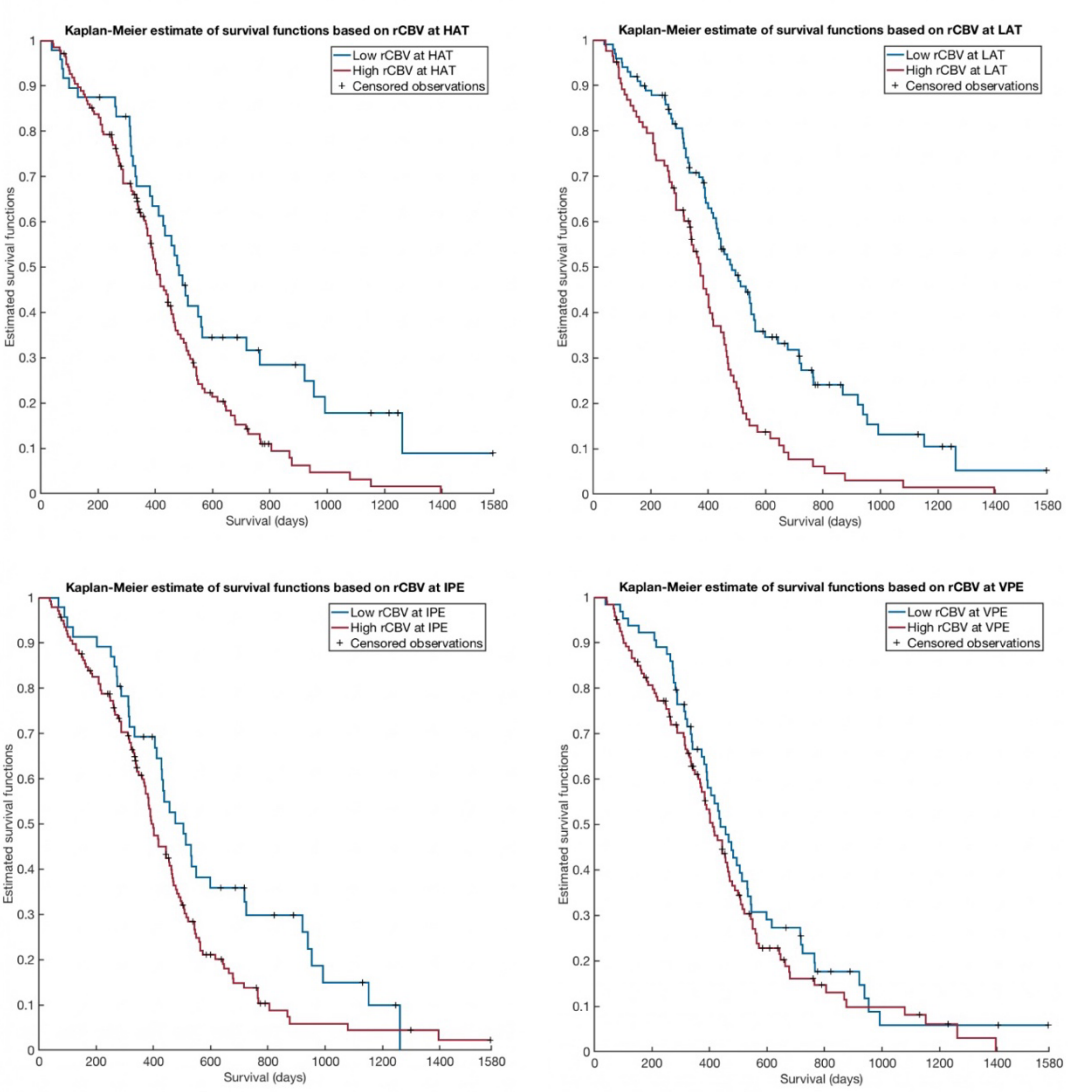

Figure 2: Kaplan-Meier estimated survival functions for the populations stratified into groups according to high or low $rCBV_{max}$ in HAT (left), LAT (center) and IPE (right) habitats.

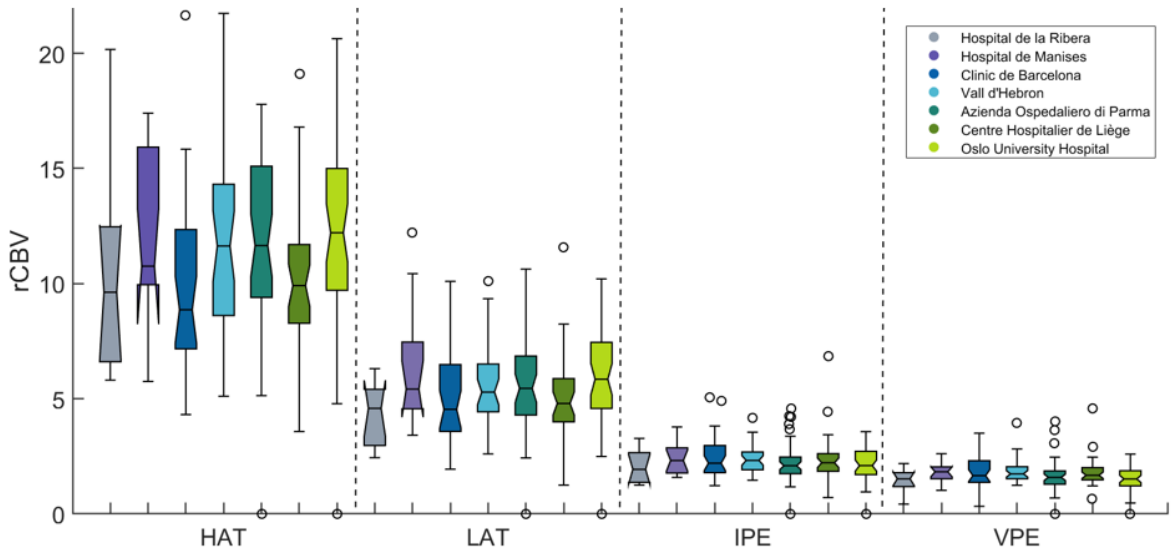

Figure 3: Boxplot of the *HTS markers* ($rCBV_{max}$ at HAT, LAT, IPE and VPE) of glioblastoma patients of each participating center.

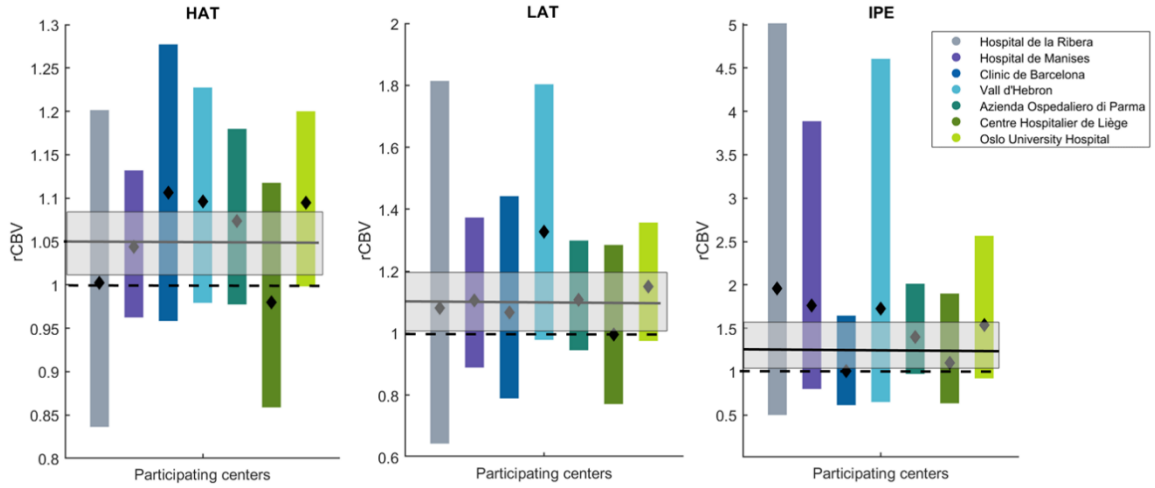

Figure 4: Plot with the Hazard Ratios (HR) and 95% Confidence Intervals (CIs) to study the association between the overall survival and the *HTS markers* at HAT, LAT and IPE for each center. The continuous black line and the grey band correspond respectively to the value of HR and CIs obtained by performing the Cox analysis with data from all centers and for each *HTS marker*. The black markers are those of the HR obtained by performing the Cox analysis with the data from each center and each *HTS marker*.

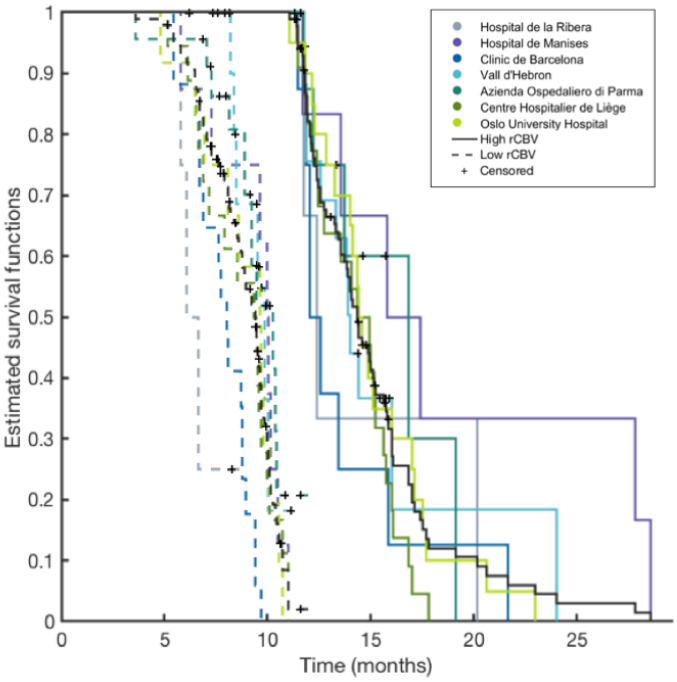

Figure 5: Kaplan-Meier estimated survival functions for the populations of each center stratified into groups according to high or low $rCBV_{max}$ in HAT, divided by the threshold calculated with the data of all the center (cut off threshold of 11.6).